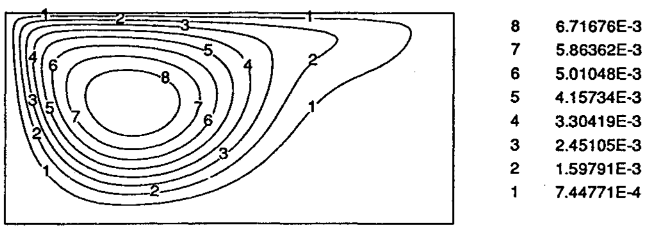

Fig. 1 Combined flowfield for parameter values $A = 2$, $Pr = 0.01$, $Ca = 0.01$, and $Re = 5.0 \times 10^3$. The cold/hot isothermal boundaries are located at $x = 0, A$, respectively. The cold corner dominates the $\mathcal{O}(1)$ flow with increasing Re.

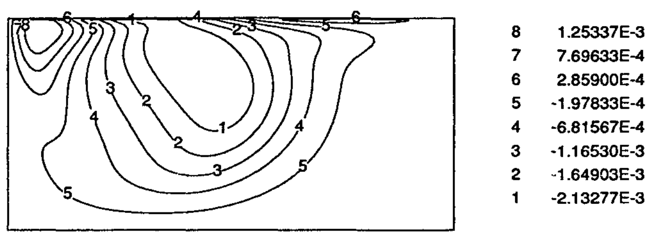

Fig. 2 $\mathcal{O}(Ca)$ flowfield for same parameter values indicated in Fig. 1. This flowfield, which is driven by the $\mathcal{O}(1)$ motion is likewise dominated by the cold corner with increasing Re.

$\mathcal{O}(1)$ flowfield, dominates the $\mathcal{O}(Ca)$ flowfield. However, in contrast to Chen and Hwu,[3] who predict a bifurcation to unsteady flow near $Re = 2.2 \times 10^2$, our results remained steady up through $Re = 5.0 \times 10^3$.

To leading order, the free surface remains flat and, thus, for these results, the free surface distortion exists only as an $\mathcal{O}(Ca)$ correction. The maximum deflection is between 0.3×10^{-3} and 0.5×10^{-3} for the parameter values considered and this small deformation clearly justifies the surface linearization approach for the values of Ca considered here. The interface that we calculated for $Re = 1000$ did not compare well in shape and maximum deflections were several orders of magnitude smaller than that reported in Ref. 3. The dependency of these deflections on A, Pr, and Re can be found elsewhere.[8]

Acknowledgments

We wish to acknowledge the support of NASA through Contract NAG3-1453 and the Pittsburgh Supercomputing Center for computational resources utilized in our work.

References

[1]Ohnishi, M., and Azuma, H., "Computer Simulation of Oscillatory Marangoni Flow," *Acta Astronautica*, Vol. 26, Nos. 8–10, 1992, pp. 685–696.

[2]Hadid, H. B., and Roux, B., "Thermocapillary Convection in Long Horizontal Layers of Low-Prandtl-Number Melts Subject to a Horizontal Temperature Gradient," *Journal of Fluid Mechanics*, Vol. 231, 1990, pp. 77–103.

[3]Chen, J. C., and Hwu, F. S., "Oscillatory Thermocapillary Flow in a Rectangular Cavity," *International Journal of Heat and Mass Transfer*, Vol. 36, No. 15, 1993, pp. 3743–3749.

[4]Liakopoulos, A., and Brown, G. W., "Thermocapillary and Natural Convection in a Square Cavity," *Surface Tension Driven Flows*, edited by G. P. Neitzel and M. K. Smith, Vol. AMD-170, American Society of Mechanical Engineers, New York, 1993, pp. 57–74.

[5]Sen, A. K., and Davis, S. H., "Steady Thermocapillary Flows in Two-Dimensional Slots," *Journal of Fluid Mechanics*, Vol. 121, 1982, pp. 163–182.

[6]Patankar, S. V., *Numerical Heat Transfer and Fluid Flow*, Hemisphere, New York, 1980.

[7]Zebib, A., Homsy, G. M., and Meiburg, E., "High Marangoni Number Convection in a Square Cavity," *Physics of Fluids*, Vol. 28, No. 12, 1985, pp. 3467–3476.

[8]Mundrane, M., Xu, J., and Zebib, A., "Thermocapillary Convection in a Rectangular Cavity with a Deformable Interface," *Advances in Space Research*, Vol. 16, No. 7, 1995, pp. 41–53.

Free Convection in a Horizontal Enclosure Partly Filled with a Porous Medium

D. Naylor*
Ryerson Polytechnic University,
Toronto, Ontario MB5 2K3, Canada
and
P. H. Oosthuizen†
Queen's University,
Kingston, Ontario K7L 3N6, Canada

Introduction

RECENTLY there has been significant interest in free convection in enclosures partly filled with a saturated porous medium. One of the motivations for studying this problem is the application to the thermal insulation of air spaces. Fibrous and particulate insulating materials can be modeled approximately as a saturated porous medium. In the present numerical study this approach is used to investigate the thermal behavior of a horizontal air gap heated from below, partly filled with a porous insulating material.

Most of the previous studies of free convection in enclosures partly filled with a porous medium have considered vertical enclosures, i.e., vertical heated/cooled walls. For the vertical enclosure, the case of no impermeable barrier between the fluid and porous medium has been studied both numerically and experimentally.[1–3] Tong and Subramanian[4] and Sathe et al.[5] have presented data for a partially filled vertical enclosure with an impermeable barrier between the fluid and porous medium. In these studies it was found that for certain conditions, completely filling an enclosure with a porous medium does not give the minimum convective heat transfer rate. These data suggest that it is possible to optimize the insulation thickness. Hence, the main purpose of the current work is to examine the effect of porous insulation depth on the convective heat transfer rate in a horizontal enclosure heated from below. Partial heating of the lower surface has also been studied as an approximate model of situations involving more localized heat sources, such as hot water pipes routed through an enclosure formed by the structural components of a building.

Problem Formulation and Solution Procedure

As shown in Fig. 1, the present study considers two-dimensional free convection in a square enclosure ($H'/W' = 1$). The central portion of the bottom surface (of length L'_H) is heated to a uniform temperature T'_h and the top of the enclosure is cooled to a uniform temperature T'_c. The enclosure is partly filled with fluid and partly filled with a layer of porous medium (of thickness S'), which is saturated with the

Received Jan. 17, 1995; revision received April 5, 1995; accepted for publication April 6, 1995.

*Assistant Professor, Department of Mechanical Engineering, 350 Victoria Street.

†Professor, Heat Transfer Laboratory, Department of Mechanical Engineering. Member AIAA.

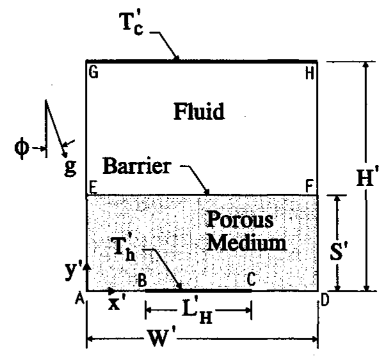

Fig. 1 Model geometry.

same fluid. At the interface between the fluid and porous medium there is an impermeable barrier that simulates the paper-backing of the insulation. This barrier is assumed to offer no resistance to heat transfer.

The flow is assumed to be steady, laminar, incompressible and two dimensional. Fluid properties are assumed to be constant, except for density, which is treated by means of the Boussinesq approximation. The standard Darcy term with the addition of the Brinkman term (viscous shear stress term) has been used to model the flow in the porous medium. It has also been assumed that for the porous medium, the convective term in the momentum equation is negligible.

The solution has been obtained in terms of the stream function ψ' and vorticity ω', using the standard definitions:

$$u' = \frac{\partial \psi'}{\partial y'} \qquad v' = -\frac{\partial \psi'}{\partial x'} \qquad \omega' = \frac{\partial v'}{\partial x'} - \frac{\partial u'}{\partial y'} \tag{1}$$

where primes (′) indicate dimensional quantities. Also, the following dimensionless variables have been defined

$$x = x'/H' \qquad y = y'/H', \qquad T = (T' - T_c')/(T_h' - T_c') \tag{2}$$

$$\psi = \psi'/\alpha_f \qquad \omega = \omega' H'^2/\alpha_f \tag{3}$$

where α_f is the thermal diffusivity of the fluid.

The governing equations for the fluid layer in terms of stream function and vorticity are standard, and for the sake of brevity, will not be reproduced here. In terms of the previous variables, the dimensionless equations for the porous medium are

$$\frac{\partial^2 \psi}{\partial x^2} + \frac{\partial^2 \psi}{\partial y^2} = -\omega \tag{4}$$

$$\frac{\nu_p}{\nu_f}\left(\frac{\partial^2 \omega}{\partial x^2} + \frac{\partial^2 \omega}{\partial y^2}\right) - \frac{\omega}{Da} = -Ra\left(\frac{\partial T}{\partial x}\cos\phi - \frac{\partial T}{\partial y}\sin\phi\right) \tag{5}$$

$$\frac{\partial^2 T}{\partial x^2} + \frac{\partial^2 T}{\partial y^2} = \frac{\alpha_f}{\alpha_p}\left(\frac{\partial \psi}{\partial y}\frac{\partial T}{\partial x} - \frac{\partial \psi}{\partial x}\frac{\partial T}{\partial y}\right) \tag{6}$$

Subscripts f and p refer to the properties in the fluid and porous medium. Note that the thermal diffusivity of the porous medium is given by $\alpha_p = k_p/\rho_f c_f$. In the above equations, the Rayleigh and Darcy numbers are defined as

$$Ra = g\beta(T_h' - T_c')H'^3/(\nu_f \alpha_f) \qquad Da = K/H'^2 \tag{7}$$

where K is the permeability of the porous medium. Referring to Fig. 1, the boundary conditions are

$$\begin{aligned} &\text{Surface DH, AG: } \psi = 0, \quad \frac{\partial \psi}{\partial x} = 0, \quad \frac{\partial T}{\partial x} = 0 \\ &\text{Surface AB, CD: } \psi = 0, \quad \frac{\partial \psi}{\partial y} = 0, \quad \frac{\partial T}{\partial y} = 0 \\ &\text{Hot surface BC: } \psi = 0, \quad \frac{\partial \psi}{\partial y} = 0, \quad T = 1 \\ &\text{Cold surface GH: } \psi = 0, \quad \frac{\partial \psi}{\partial y} = 0, \quad T = 0 \end{aligned} \tag{8}$$

The following conditions were applied at the impermeable barrier:

$$\psi = 0, \qquad \frac{\partial \psi}{\partial y} = 0, \qquad \left.\frac{\partial T}{\partial y}\right|_f = \left(\frac{k_p}{k_f}\right)\left.\frac{\partial T}{\partial y}\right|_p \tag{9}$$

The governing equations have been solved using a Galerkin finite element method (FEM). Triangular elements with linear interpolation functions were used. The resulting simultaneous equations were solved iteratively using successive overrelaxation. For the two limiting cases of $S'/H' = 0$ and $S'/H' = 1$, comparisons were made with previous numerical solutions. For the fluid-filled cavity heated from below ($S'/H' = 0$) the average Nusselt number results were within 3% of those of Ozoe and Sayama.[6] For the porous medium filled cavity ($S'/H' = 1$), the results were within about 2% of those of Prasad et al.[7] for a vertical heated cavity ($\phi = 90$ deg). Calculations were performed on a nonuniform mesh with 41 × 37 nodes. Grid testing showed that the average Nusselt number data are grid independent to better than 1%. The results are presented in terms of the cold wall average Nusselt number defined as

$$\overline{Nu_c} = \frac{qH'}{k_f(T_h' - T_c')W'} \tag{10}$$

where q is the overall heat transfer rate.

Results

Calculations have been made over the following ranges: $10^3 \leq Ra \leq 3 \times 10^5$, $Da = 10^{-4}, 10^{-3}$, $0 \leq S'/H' \leq 1$, $L_H'/W' = \frac{1}{3}, \frac{2}{3}$, and 1. The conductivity ratio has been taken as $k_p/k_f = 1$. This condition is approximately satisfied by some types of insulating materials (e.g., glass fiber). The viscosity ratio has been taken as $\nu_p/\nu_f = 1$, which has been found to provide good agreement with experimental data. Results have been obtained for a square enclosure $H'/W' = 1$, and a Prandtl number of $Pr = 0.7$.

Preliminary calculations revealed that the flow patterns were very sensitive to small angles of inclination. In many cases, small angles of inclination ($\phi = 1$ deg) caused the flow patterns to change drastically compared to those of the perfectly horizontal case ($\phi = 0$ deg). Often the flow would abruptly lose symmetry about the vertical centerline of the enclosure. For this reason the present calculations were run at an inclination angle of $\phi = 1$ deg. This slight inclination introduces a consistent, small, asymmetric disturbance that may yield more realistic predictions.

Figure 2 shows the effect of the depth of the porous layer on the average Nusselt number for $Ra = 3 \times 10^5$ and $Da = 10^{-4}$. The flow in the porous media is very weak ($RaDa = 30$) and the heat transfer in the porous layer occurs almost by pure conduction, even for $S'/H' = 1$. Hence, as S'/H' increases, the decreasing strength of the convection in the fluid layer causes the average Nusselt number to decrease

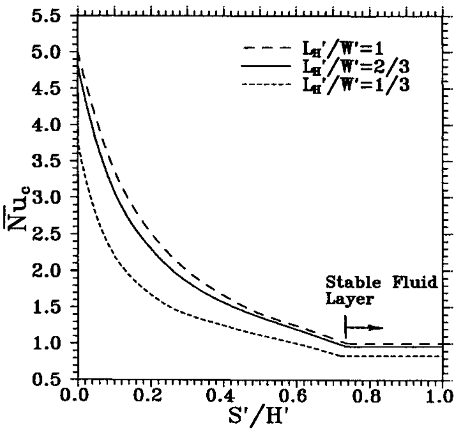

Fig. 2 Effect of the depth of the porous layer (S'/H') on the average Nusselt number for $Ra = 3 \times 10^{-5}$ and $Da = 10^{-4}$.

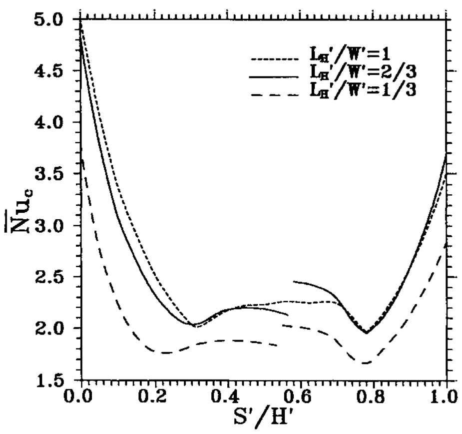

Fig. 3 Effect of the depth of the porous layer (S'/H') on the average Nusselt number for $Ra = 3 \times 10^5$ and $Da = 10^{-3}$.

rapidly. At $S'/H' \approx 0.73$, the depth of the fluid layer and the temperature difference across the fluid layer are reduced sufficiently to completely stabilize the fluid. Applying the well-known stability criterion for a fluid layer uniformly heated from below (effective Rayleigh number $Ra_{\text{eff}} \leq 1706$) indicates that the fluid layer will be stable for $S'/H' \geq 0.725$, which is in close agreement with the numerical prediction. Note that the fluid layer stability limit is almost unaffected by partial wall heating; this is because the porous layer is sufficiently thick that the horizontal temperature gradients at the barrier (which tend to destabilize the fluid), are small.

Figure 3 shows the effect of the porous layer depth on the average Nusselt number for $Ra = 3 \times 10^5$ and $Da = 10^{-3}$ ($RaDa = 300$). The general shape of the Nusselt number curves for $L'_H/W' = \frac{1}{3}, \frac{2}{3}$, and 1 are similar. As expected, the heat transfer rate is the highest for $S'/H' = 0$. As S'/H' increases, the average Nusselt number initially decreases because there is almost no convective motion in the thin porous layer. As S'/H' increases further, the Nusselt number reaches a local minimum and starts to increase as the convection in the porous layer strengthens. For $L'_H/W' = \frac{1}{3}$ and $L'_H/W' = \frac{2}{3}$, a discontinuity in the Nusselt number variation was found at approximately $S'/H' = 0.55$. At $S'/H' \approx 0.55$, the decreasing depth of the fluid layer causes the flow to change abruptly from an asymmetric unicellular pattern in the fluid, to a two-cell pattern that is nearly symmetric about the vertical centerline of the enclosure. For thicker porous layers ($S'/H' > 0.55$), the heat transfer decreases because of the weakening convective motion in the narrowing fluid-side gap. However, for S'/H' greater than about $S'/H' = 0.78$, the thermal resistance of the near stagnant fluid layer becomes the dominant

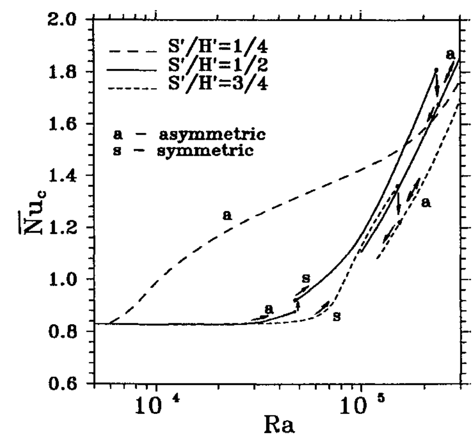

Fig. 4 Variation of the cold wall average Nusselt number with Rayleigh number for $Da = 10^{-3}$, $L'_H/W' = \frac{1}{3}$.

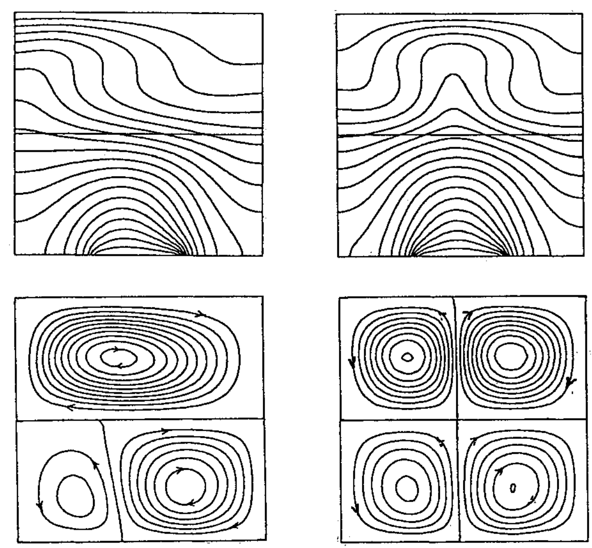

Fig. 5 Streamline and isotherm contours for the two solutions at $Da = 10^{-3}$, $Ra = 10^5$, $L'_H/W' = \frac{1}{3}$, $S'/H' = \frac{1}{2}$ ($\Delta T = 0.05$, $\Delta\psi_p = 0.2$, $\Delta\psi_f = 0.5$).

effect and the Nusselt number increases rapidly as $S'/H' \rightarrow 1.0$. Note that the heat transfer rate is close to the minimum when the cavity is only about one-third filled.

Figure 4 shows the variation of the average Nusselt number with Rayleigh number for various depths of the porous layer at $Da = 10^{-3}$. Note that for $S'/H' = \frac{1}{2}$ and $S'/H' = \frac{3}{4}$, there are discontinuities in the Nusselt number variations. These discontinuities are caused by an abrupt change in the flow pattern (particularly in the fluid layer) from a symmetric pattern to an asymmetric pattern, or vice versa. The curve segments are labeled either "s" or "a," denoting whether a near symmetric or strongly asymmetric flow pattern exists. It is also shown in Fig. 4 that dual solution regions exist. These dual solution regions were obtained from different initial values in the iterative solution procedure. For example, for $S'/H' = \frac{1}{2}$, solutions with asymmetric flow patterns could only be obtained for $Ra < 2.0 \times 10^5$ when solutions at a higher Rayleigh number (with asymmetric flow patterns) were used as the initial values for the iterative procedure. Figure 5 shows the isotherm and streamline contours for the two solutions that were obtained for $Da = 10^{-3}$, $Ra = 10^5$, $L'_H/W' = \frac{1}{3}$, and $S'/H' = \frac{1}{2}$. It should be noted that the current results are based on the steady-state equations. The governing equations must be solved in transient form to precisely examine the bifurcation phenomena that seems to exist for this geometry.

References

[1]Song, M., and Viskanta, R., "Natural Convection Flow and Heat Transfer Between a Fluid Layer and an Anisotropic Porous Layer within a Rectangular Enclosure," *Heat Transfer in Enclosures*, American Society of Mechanical Engineers, HTD-Vol. 177, 1991, pp. 1–12.

[2]Arquis, E., Caltagirone, J. P., and Langlais, C., "Natural Convection in Cavities Partially Filled with Permeable Porous Materials," *Proceedings of the 8th International Heat Transfer Conference*, Vol. 5 (San Francisco, CA), 1986, pp. 2653–2658.

[3]Beckermann, C., Ramadhyani, S., and Viskanta, R., "Natural Convection Flow and Heat Transfer Between a Fluid Layer and a Porous Layer Inside a Rectangular Enclosure," *Journal of Heat Transfer*, Vol. 109, May 1987, pp. 363–370.

[4]Tong, T. W., and Subramanian, E., "Natural Convection in Rectangular Enclosures Partially Filled with a Porous Medium," *International Journal of Heat and Fluid Flow*, Vol. 7, March 1986, pp. 3–10.

[5]Sathe, S. B., Tong, T. W., and Faruque, M. A., "Experimental Study of Natural Convection in a Partially Porous Enclosure," *Journal of Thermophysics and Heat Transfer*, Vol. 1, 1987, pp. 260–267.

[6]Ozoe, H., Sayama, H., and Churchill, S. W., "Natural Convection in an Inclined Square Cavity," *International Journal of Heat and Mass Transfer*, Vol. 17, 1974, pp. 401–406.

[7]Prasad, V., Lauriat, G., and Kladias, N., "Non-Darcy Natural Convection in a Vertical Porous Cavity," *Heat and Mass Transfer in Porous Media*, Elsevier, New York, 1992, pp. 293–314.

Forced Convection in Ducts with a Boundary Condition of the Third Kind

R. C. Xin,* Z. F. Dong,† and M. A. Ebadian‡
Florida International University, Miami, Florida 33199
and
W. Q. Tao§
Xi'an Jiatong University,
Xi'an, Shaanxi 710049, China

Introduction

LAMINAR flow of an incompressible fluid in ducts, such as a circular pipe, parallel plates, rectangular ducts, isosceles triangular ducts, and hexagonal ducts is mainly encountered in compact heat exchangers. Numerous investigations have been conducted and the correlations for the friction factor and heat transfer coefficient can be found in handbooks.[1] However, these solutions were obtained for the case of forced convection heat transfer inside the duct subject to the first kind (uniform wall temperature) or second kind (uniform wall heat flux) of boundary conditions, which are the two extreme cases of the third kind when the Biot number approaches infinity or zero. The convection heat transfer from the ambient fluid to the duct can be represented properly by the third kind of thermal boundary condition. In some cases, the third kind of thermal boundary condition also refers to the case where the duct has a finite thermal resistance normal to the wall.[2] Only a few papers have been published on forced convection heat transfer in circular and noncircular ducts with the thermal boundary condition of the third kind. Most of the work focused on the developing region of the circular pipe,[3–5] the flat channel,[6] and the rectangular duct.[7] The forced convection heat transfer of fully developed flow in the circular pipe can be found in numerical work.[8] Convection heat transfer in the noncircular isosceles triangular and hexagonal ducts with the third kind of thermal boundary condition has not as yet been reported. Although the solution for the heat transfer of slug flow in the entrance region of a circular pipe[9] and a rectangular duct[10] has been obtained for the first and second kinds of thermal boundary conditions, the solution for the third kind of thermal boundary condition still needs to be studied. The analytical or numerical solution will be studied for the case of the third kind of thermal boundary condition for both slug and fully developed flows. The slug flow often occurs in fluids with a small Prandtl number, corresponding to the entrance flow.

Analysis

Consideration is given mainly to the steady laminar flow in circular and noncircular ducts, such as flow in parallel plates, the rectangular duct, the isosceles triangular duct, or the hexagonal duct. The fluid flow is assumed as hydrodynamically and thermally fully developed and the thermal properties of the fluid are independent of temperature. In addition, heat generation and viscous dissipation of the fluid are not taken into account. The third kind of boundary condition is imposed for all of the ducts considered here. Therefore, the heat transfer of fluid inside the duct can be described by

$$\rho C_p u \frac{\partial T}{\partial z} = k\left(\frac{\partial^2 T}{\partial x^2} + \frac{\partial^2 T}{\partial y^2}\right) \tag{1}$$

with a boundary condition at the wall

$$-k \frac{\partial T}{\partial n}\bigg|_w = h(T - T_\infty)|_w \tag{2}$$

where ρ, C_p, and k are density, specific heat, and the thermal conductivity of the fluid, respectively; u and T are velocity and temperature; x and y are coordinates in the cross section; $\partial T/\partial z$ is the temperature gradient in the axial direction; h is the heat transfer coefficient of the ambient fluid; and T_∞ is the temperature of the ambient fluid.

After introducing dimensionless variables[8]

$$X = x/l, \qquad Y = y/l, \qquad U = u/u_m, \qquad N = n/l$$
$$\theta = (T - T_\infty)/(T_b - T_\infty), \qquad Bi = h \cdot l/k \tag{3}$$
$$Pe = \rho C_p u_m l/k, \qquad \lambda = -\frac{1}{T_b - T_\infty}\frac{\mathrm{d}(T_b - T_\infty)}{\mathrm{d}z}$$

Eqs. (1) and (2) become

$$\frac{\partial^2\theta}{\partial X^2} + \frac{\partial^2\theta}{\partial Y^2} + \lambda Pe U\theta = 0 \tag{4}$$

$$\frac{\partial\theta}{\partial N}\bigg|_w = -Bi\theta|_w \tag{5}$$

In Eqs. (3–5), Bi is the Biot number, Pe is the Peclet number, and u_m and T_b are the mean velocity and bulk temperature of the fluid, respectively. l is the characteristic length of the duct that is defined in Table 1 for each duct. It is noted that

Received Oct. 3, 1994; revision received May 19, 1995; accepted for publication May 22, 1995.

*Graduate Student, Department of Mechanical Engineering. Student Member AIAA.

†Visiting Assistant Professor, Department of Mechanical Engineering. Member AIAA.

‡Professor and Chairperson, Department of Mechanical Engineering.

§Professor, College of Energy and Power Engineering.